AGU PUBLICATIONS

JGR

Journal of Geophysical Research: Space Physics

RESEARCH ARTICLE
10.1002/2016JA022968

**Key Points:**
- Long-lasting QP event observed simultaneously by the DEMETER spacecraft and on the ground
- Frequency-time structure observed by both instruments is the same, but there is a time delay between detection of individual QP elements
- When QP event intensity increases, there is also an increase of the amplitude of ULF pulsations measured on the ground at high latitudes

**Correspondence to:**
F. Němec,
frantisek.nemec@gmail.com

**Citation:**
Němec, F., B. Bezděková, J. Manninen, M. Parrot, O. Santolík, M. Hayosh, and T. Turunen (2016), Conjugate observations of a remarkable quasiperiodic event by the low-altitude DEMETER spacecraft and ground-based instruments, *J. Geophys. Res. Space Physics*, *121*, 8790–8803, doi:10.1002/2016JA022968.

Received 18 MAY 2016
Accepted 9 SEP 2016
Accepted article online 14 SEP 2016
Published online 28 SEP 2016



# Conjugate observations of a remarkable quasiperiodic event by the low-altitude DEMETER spacecraft and ground-based instruments

**F. Němec[1], B. Bezděková[1], J. Manninen[2], M. Parrot[3], O. Santolík[1,4], M. Hayosh[4], and T. Turunen[2]**

[1]Faculty of Mathematics and Physics, Charles University in Prague, Prague, Czech Republic, [2]Sodankylä Geophysical Observatory, Sodankylä, Finland, [3]LPC2E/CNRS, Orléans, France, [4]Institute of Atmospheric Physics, Czech Academy of Sciences, Prague, Czech Republic

**Abstract** We present a detailed analysis of a long-lasting quasiperiodic (QP) event observed simultaneously by the low-altitude DEMETER spacecraft and on the ground by the instrumentation of the Sodankylä Geophysical Observatory, Finland. The event was observed on 26 February 2008. It lasted for several hours, and it was detected both in the Northern and Southern Hemispheres. The time intervals when the event was observed on board the satellite and/or on the ground provide us with an estimate of the event dimensions. When the event is detected simultaneously by the satellite and on the ground, the observed frequency-time structure is generally the same. However, the ratio of detected intensities varies significantly as a function of the spacecraft latitude, indicating the wave guiding along the plasmapause. Moreover, there is a delay as large as about 13 s between the times when individual QP elements are detected by the spacecraft and on the ground. This appears to be related to the azimuthal separation of the instruments, and it is highly relevant to the identification of a possible source mechanism. We suggest that it is due to an azimuthally propagating ULF wave which periodically modulates the azimuthally extended source region. Finally, we find that at the times when the intensity of the QP event suddenly increases, there is a distinct increase of the amplitude of Alfvénic ULF pulsations measured on the ground at high latitudes. This might indicate that the source region is located at L shells larger than about 7.1.

## 1. Introduction

Whistler mode electromagnetic waves in the very low frequency (VLF) range observed in the inner magnetosphere sometimes exhibit a nearly periodic modulation of the wave intensity. The modulation period may be from some tens of seconds up to a few minutes, and the events typically occur in the frequency range from about 0.5 up to 4 kHz [*Carson et al.*, 1965; *Sato and Kokubun*, 1980; *Sato and Fukunishi*, 1981; *Smith et al.*, 1998]. Such electromagnetic waves are usually called quasiperiodic (QP) emissions. Although the emissions were extensively studied for already a few decades, their generation mechanism still has not been satisfactorily explained.

QP emissions are known to be primarily daytime phenomenon [*Morrison et al.*, 1994; *Engebretson et al.*, 2004; *Hayosh et al.*, 2014]. Historically, they were classified using ground-based measurements into two classes, called "QP emissions type 1" and "QP emissions type 2" [*Kitamura et al.*, 1969; *Sato et al.*, 1974]. The used criterion was whether or not coincident ultralow frequency (ULF) magnetic field pulsations with a period comparable to the modulation period of QP emissions were observed on the ground. If such pulsations were observed, the events were classified as QP emissions type 1, if such pulsations were absent, the events were classified as QP emissions type 2.

As for possible generation mechanisms of QP events, two principally different scenarios were suggested. The first one, inspired by the ULF magnetic field pulsations observed along with QP emissions type 1, is based on the idea of resonant conditions in the source region being periodically modulated by a compressional ULF wave [*Chen*, 1974; *Sato and Fukunishi*, 1981; *Sazhin*, 1987]. A theoretical analysis suggests that already rather minor ULF magnetic field pulsations might result in significant modulations of the wave growth rate [*Kimura*, 1974]. However, one should note that although this generation mechanism assumes the presence of a compressional ULF wave, magnetic field pulsations observed on the ground are typically Alfvénic,

i.e., noncompressional. Nevertheless, it is possible that the compressional pulsations responsible for the QP modulation of the VLF wave intensity are limited only to the narrow equatorial region, and they are mode converted to Alfvénic pulsations at larger geomagnetic latitudes [*Němec et al.*, 2013a]. This possibility seems to be partly supported by observations, as out of the three QP events observed by the Cluster spacecraft close to the geomagnetic equator during the close separation campaign in summer 2013, compressional ULF magnetic field pulsations were observed in two events [*Němec et al.*, 2014].

The second suggested possible generation mechanism is based on the periodic wave generation in the regime of relaxation oscillations [*Bespalov and Trakhtengerts*, 1976; *Davidson*, 1979]. A rigorous kinetic model involving a flow cyclotron maser and taking into account variable shapes of the wave spectrum was subsequently developed [*Trakhtengerts et al.*, 1986; *Demekhov and Trakhtengerts*, 1994; *Pasmanik et al.*, 2004a]. The model was also applied to explain some of the satellite observations of QP emissions [*Pasmanik et al.*, 2004b]. As this mechanism does not require any modulating ULF wave, it could be used to explain QP emissions of type 2. Nevertheless, it is important to note that the classification of QP emissions into type 1 and type 2 becomes significantly less clear when the satellite data are used in place of ground measurements [*Tixier and Cornilleau-Wehrlin*, 1986]. In fact, it appears that both types of QP emissions might have the same generation mechanism, and their distinction is thus rather questionable [*Sazhin and Hayakawa*, 1994].

Multipoint measurements of the same event are crucial to distinguish between spatial and temporal variations of the phenomenon. Such observations are typically rather difficult to gather, and a detailed analysis of only a few such events has been performed up to now [*Němec et al.*, 2013a, 2013b, 2014; *Titova et al.*, 2015; *Němec et al.*, 2016]. Moreover, while ground-based measurements can provide important information about temporal variations of an event [*Smith et al.*, 1991; *Manninen et al.*, 2012, 2013, 2014a, 2014b], spacecraft measurements are crucial to obtain the information about the event spatial variability. It is thus beneficial to combine the two types of measurements. When multipoint observations of a QP event are available, they generally show that principally the same QP modulation is observed over a large spatial region [*Němec et al.*, 2013a, 2013b, 2014; *Titova et al.*, 2015]. However, the times when individual QP elements (intensity maxima) occur at different locations can differ by a few seconds. This can be likely explained by the unducted wave propagation of the emissions and one of the observers being located closer to the source than the other [*Němec et al.*, 2014; *Martinez-Calderon et al.*, 2016]. We note, however, that these time delays were obtained for two points located at principally the same magnetic local time (MLT), separated by about $0.5R_E$ radially. The situation may be rather different when the azimuthal distance is concerned. Specifically, *Němec et al.* [2016] used observations by multiple spacecraft to identify the time delays as large as about 15 s for the azimuthal separations of the spacecraft about 25° in longitude. Curiously, they also reported that when a QP event is observed simultaneously on the dawnside and on the duskside, its modulation period on the duskside is about twice larger.

In any case, QP emissions are believed to be generated in the equatorial region, close to the plasmapause or at even larger radial distances [*Sato and Kokubun*, 1980; *Morrison*, 1990]. Detailed wave analysis of satellite observations of these emissions [*Němec et al.*, 2013a; *Titova et al.*, 2015; *Hayosh et al.*, 2016] as well as multistation ground-based measurements [*Gołłkowski and Inan*, 2008] indicate that QP emissions propagate unducted. However, there is an indirect evidence that the emissions may be guided along the plasmapause boundary when propagating down to the low altitudes [*Hayosh et al.*, 2016]. A ray tracing analysis of such a plasmapause guiding suggests that the waves would be deviated toward lower geomagnetic latitudes at altitudes of a few thousands of kilometers [*Inan and Bell*, 1977].

We present a detailed analysis of an exceptional long-lasting QP event observed simultaneously by the low-altitude DEMETER satellite and by the ground-based instrumentation of the Sodankylä Geophysical Observatory (SGO), Finland. The instrumentation is described in section 2. The obtained results are presented in section 3, and they are discussed in section 4. Finally, section 5 presents a brief summary of the main results.

## 2. Data Set

DEMETER was a low-altitude spacecraft which operated between 2004 and 2010. It had an approximately circular orbit with an altitude of about 700 km. The orbit was nearly Sun synchronous, i.e., the measurements were always performed close to either 10:30 LT or 22:30 LT. The instruments on board performed both wave and particle measurements. These measurements were continuous at geomagnetic latitudes lower than 65°.

In the VLF range that we are interested in, frequency-time spectrograms of power spectral density of one electric and one magnetic field component were calculated on board. These spectrograms cover the frequency range up to 20 kHz. The frequency resolution is about 19.53 Hz, and the time resolution is about 2 s. As the magnetic field data suffer from a significant amount of interferences in the frequency range 1–8 kHz, only electric field data will be used in the present study [*Berthelier et al.*, 2006a].

The wave measurements on the ground are performed at the Kannuslehto station (67.74°N, 26.27°E, $L \approx 5.4$) operated by the Sodankylä Geophysical Observatory (SGO), Sodankylä, Finland. Two orthogonal magnetic loop antennas oriented in the north-south and east-west directions are used. The size of the antennas is 10 by 10 m, and their effective area is 1000 $m^2$. The emissions are band-pass filtered in the frequency range 0.2–39 kHz and sampled with the sampling frequency of 78,125 Hz. The receiver has a wide dynamic range (up to 120 dB), and an exceptional sensitivity (approximately 0.1 fT). A more detailed description of the instrument was given by *Manninen* [2005]. The magnetic field intensities are calibrated using the method described by *Fedorenko et al.* [2014]. Fast Fourier transform (FFT) is performed to obtain power spectral densities of magnetic field fluctuations. These are then converted to power spectral densities of electric field fluctuations by multiplying by the factor $c^2$, where $c$ is the speed of light. This is done in order to allow a direct intensity comparison with the DEMETER electric field data.

Ground-based magnetometers of the IMAGE magnetometer chain in Finland and in Northern Scandinavia provide continuous measurements of the three components of the ambient magnetic field [*Tanskanen*, 2009]. The time resolution of these measurements is 10 s. An important point is that the time resolution is good enough to analyze the time scales shorter than the modulation period of the analyzed QP event; i.e., it allows us to analyze magnetic field pulsations detected on the ground and possibly related to the occurrence of the QP event.

## 3. Results

The QP event analyzed in this paper was observed by the ground-based instrumentation at Kannuslehto on 26 February 2008 between about 01:30 and 21:00 UT. However, it was not observed continuously, but with gaps between about 06:10 and 10:40 UT and 13:20 and 17:00 UT. Moreover, the event was observed in eight consecutive daytime half-orbits of the DEMETER spacecraft, and also in two nighttime half-orbits. An overview of the situation is shown in Figure 1. It shows a map of locations in geomagnetic coordinates where the event was observed. The location of the Kannuslehto station (Finland) is shown by the thick cross (geomagnetic longitude of 119.96°, geomagnetic latitude of 64.36°). The individual curves shown in the figure correspond to the projections of the DEMETER orbits relevant for the event observation. The thick red curves show the positions of the spacecraft at the times when QP emissions were observed simultaneously by DEMETER and by the Kannuslehto station. The thin orange curves show the positions of the satellite at the times when QP emissions were observed only on the ground. Finally, the thick blue curves show the satellite positions at the times when QP emissions were observed by DEMETER, but not on the ground. The Universal Time of the beginning of each satellite half-orbit is shown. Note that during the daytime half-orbits, the satellite moves from north-east to south-west, while during the nighttime half-orbits, the satellite moves from south-east to north-west. The parts of the satellite orbits where the emissions were particularly well pronounced both in DEMETER and ground-based data are marked by capital letters. These will be used for a detailed conjugate analysis. It can be seen that at the times when both DEMETER and Kannuslehto observe the emissions, DEMETER can be as far as 102° in longitude. Curiously, there are times when the satellite is very close to the Kannuslehto station, but the QP emissions are observed only by DEMETER.

A frequency-time spectrogram of 90 min of observations at Kannuslehto station is shown in Figure 2. The wave power spectral densities expressed in electric field units are color coded according to the scale on the right-hand side. The data were measured on 26 February 2008 between 10:40 UT and 12:10 UT. QP emissions can be identified at frequencies between about 1000 and 2500 Hz. While in the lower frequency part the QP emissions are hiss like and incoherent, individual QP elements are well pronounced at frequencies above about 1500 Hz. Although these elements are not so intense in the beginning and at the end of the plotted time interval, their intensity gradually increases toward the center.

Figure 3 shows a direct comparison between frequency-time spectrograms obtained by the DEMETER spacecraft and Kannuslehto station during the time intervals marked "A" and "B" in Figure 1. Figure 3a shows a frequency-time spectrogram of power spectral density of electric field fluctuations measured by the

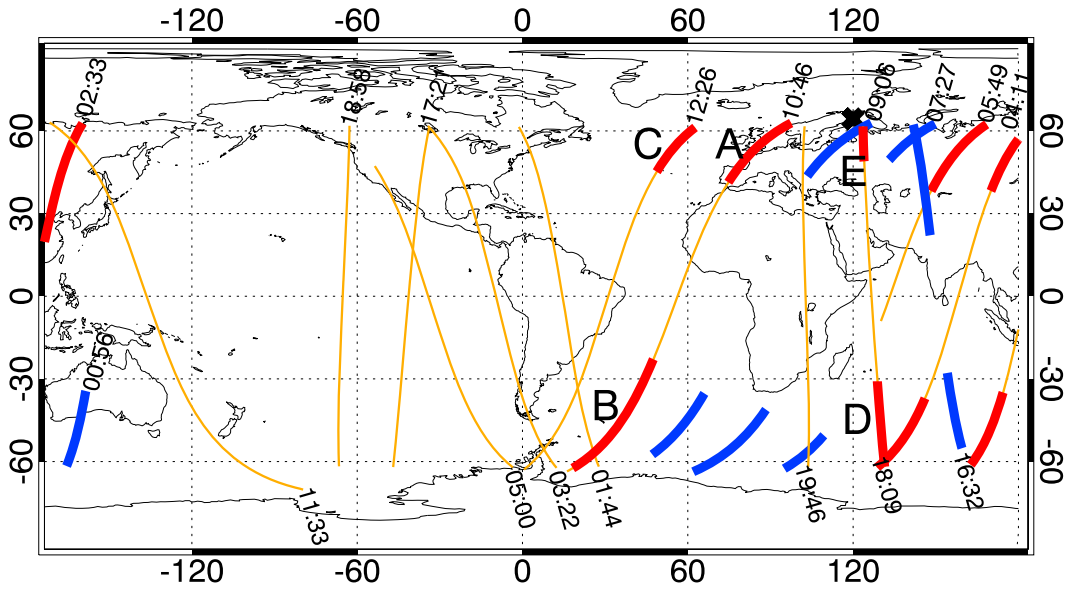


**Figure 1.** Map of event locations in geomagnetic coordinates. The location of the Kannuslehto station where the ground-based measurements were performed is shown by the thick cross (geomagnetic longitude 119.96°, geomagnetic latitude 64.36°). The thick red curves show the positions of the DEMETER spacecraft at the times when QP emissions were observed simultaneously by the satellite and on the ground. The thin orange curves show the positions of the DEMETER spacecraft at the times when QP emissions were observed only on the ground. The thick blue curves show the satellite positions at the times when QP emissions were observed exclusively by DEMETER. The start time of each satellite half-orbit is shown at its beginning. Note that the daytime half-orbits are north-east to south-west, while the nighttime half-orbits are south-east to north-west. The capital letters mark parts of the satellite orbits, where the emissions were particularly well pronounced both in DEMETER and ground-based data. These are used for further conjugate analysis.

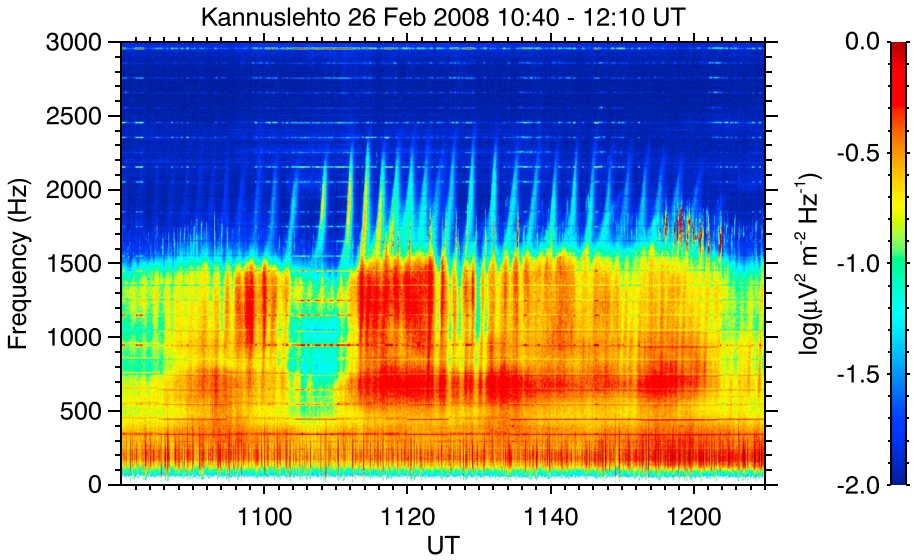


**Figure 2.** Frequency-time spectrogram of power spectral density of magnetic field fluctuations (recalculated to electric field units using the $c^2$ factor, see text for more details) measured at the Kannuslehto station on 26 February 2008 between 10:40 UT and 12:10 UT. Wave intensities are color coded according to the scale on the right-hand side. QP emissions can be seen at frequencies between about 1000 Hz and 2500 Hz. Individual QP elements are particularly well pronounced at frequencies larger than about 1500 Hz. The QP elements are rather weak in the beginning and at the end of the time interval, but their intensity gradually increases toward the center.

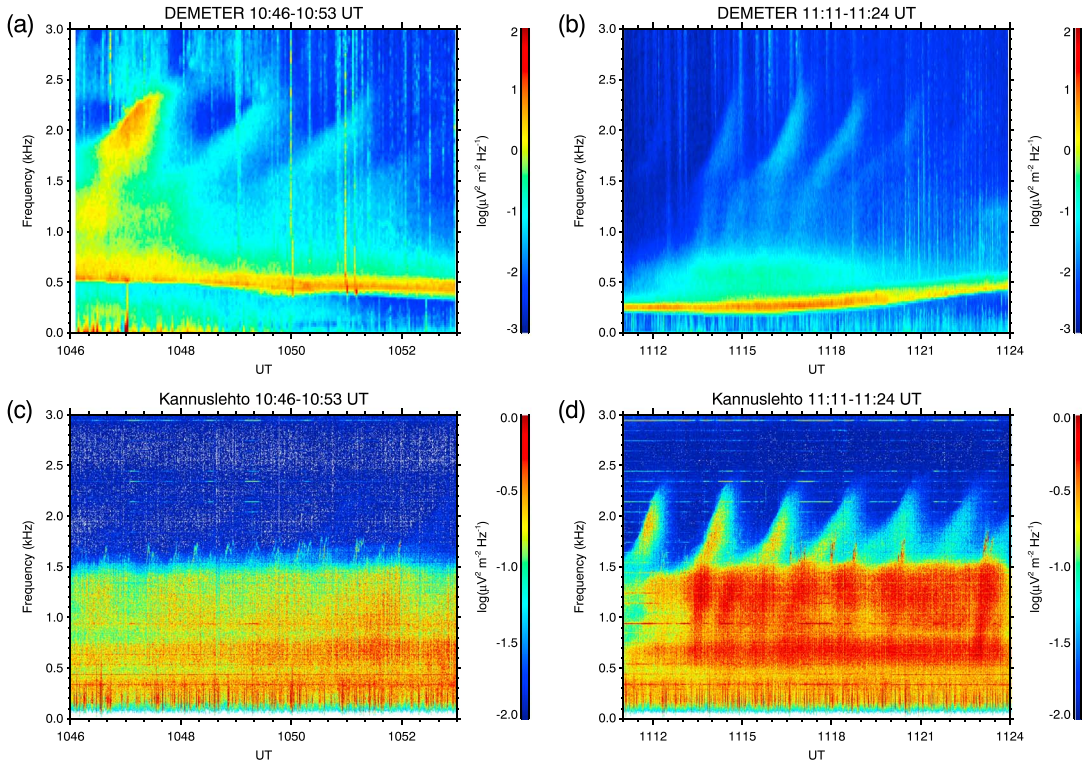


**Figure 3.** (a) Frequency-time spectrogram of power spectral density of electric field fluctuations measured by the DEMETER spacecraft on 26 February 2008 between 10:46 UT and 10:53 UT (orbit part A in Figure 1). (b) Frequency-time spectrogram of power spectral density of electric field fluctuations measured by the DEMETER spacecraft on 26 February 2008 between 11:11 UT and 11:24 UT (orbit part B in Figure 1). (c) The same as Figure 3a but for Kannuslehto magnetic field measurements. (d) The same as Figure 3b but for Kannuslehto magnetic field measurements.

DEMETER spacecraft on 26 February 2008 between 10:46 UT and 10:53 UT. Frequency-time spectrogram of the wave intensity measured at the same time by the Kannuslehto station is shown in Figure 3c. This time interval corresponds to the time interval marked as A in Figure 1; i.e., DEMETER was rather close to Kannuslehto and in the same hemisphere. Figure 3b shows a frequency-time spectrogram of power spectral density of electric field fluctuations measured by the DEMETER spacecraft on 26 February 2008 between 11:11 UT and 11:24 UT. Frequency-time spectrogram of the wave intensity measured at the same time by the Kannuslehto station is shown in Figure 3d. This time interval corresponds to the time interval marked B in Figure 1; i.e., DEMETER was located in the opposite hemisphere than Kannuslehto and by 72–102° westward.

Individual QP elements can be well distinguished in Figures 3a, 3b, and 3d. The QP elements in Figure 3c are much weaker, and their low intensity nearly prevents their observation in the used color scale. Although the lower frequency parts of the spectrograms differ significantly between DEMETER and Kannuslehto, individual QP elements seem to reasonably agree, both in the frequency range and in the shape. There appear to be some fine-scale differences in the inner structure of individual QP elements, but the limited frequency-time resolution of the DEMETER data does not allow us to investigate these in great detail.

It is curious that the intensity of the QP emissions is so much different between DEMETER and Kannuslehto during the interval A, when DEMETER is rather close. This is principally the same phenomenon as already seen in the overall map in Figure 1, and it will be discussed in more detail in section 4. Moreover, it can be seen that while the intensity of individual QP elements remains about the same in Figure 3d, the intensity of QP elements observed by DEMETER in Figure 3b varies considerably. This is related to the latitudinal movement of the satellite, and it will be discussed in more detail later.

It is interesting to compare the exact timing of individual QP elements between DEMETER and Kannuslehto and to determine whether there is a detectable time delay between the two instruments or not. This is done in Figure 4. We selected the frequency range between 1900 and 2000 Hz, and we plotted the power spectral density in this frequency range as a function of time. Note that principally the same result is obtained

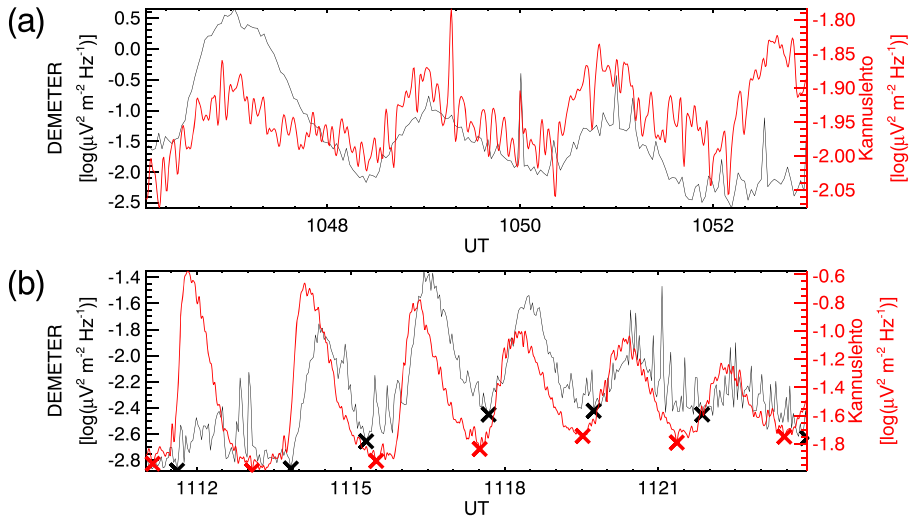


**Figure 4.** (a) Time dependence of the power spectral density in the frequency range of 1900–2000 Hz corresponding to the time interval from Figures 3a and 3c. The black curve and the scale on the left-hand side correspond to the data measured by the DEMETER spacecraft. The red curve and the scale on the right-hand side corresponds to the ground-based data measured at the Kannuslehto station. (b) The same as Figure 4a but for the time interval from Figures 3b and 3d. The black and the red crosses mark the times of the beginnings/ends of individual QP elements as observed by DEMETER and Kannuslehto, respectively.

independently on the chosen frequency band, as long as it is the frequency band which contains the QP elements. Figures 4a and 4b correspond to the time intervals A and B, respectively; i.e., they are frequency cuts from Figures 3a and 3c and 3b and 3d. The black curves and the scales on the left-hand side correspond to the data measured by the DEMETER spacecraft. The data measured at the Kannuslehto station are depicted using the red curves and the scales on the right-hand side. The red curve in Figure 4a is quite noisy, as the wave intensity detected by Kannuslehto during this time interval was rather low. Nevertheless, the four peaks in the wave intensity corresponding to the four distinct QP elements can be identified. The times when these intensity peaks occur in DEMETER and Kannuslehto data are roughly the same, but a small systematic time delay might be hidden in the noise. On the other hand, there is a clear time delay observable in Figure 4b. The red curve is systematically shifted toward earlier times as compared to the black curve; i.e., the individual QP elements are detected first by the Kannuslehto station, and then, with a distinct time delay, by the DEMETER spacecraft. The black and the red crosses in Figure 4b show the beginning/ending times of individual QP elements as observed by DEMETER and Kannuslehto, respectively. These were determined as the intensity minima in between the QP elements, and they will be used in the further analysis.

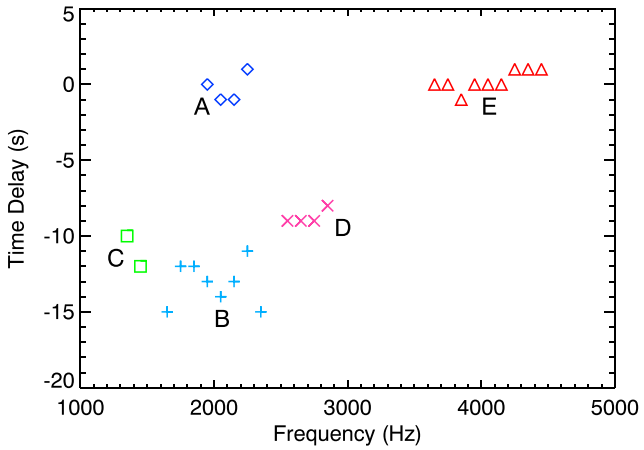


**Figure 5.** Time delays between the detection of individual QP elements by DEMETER and the Kannuslehto station as a function of frequency. The data points marked by the same symbols of the same color were obtained for the same time interval, but at different frequency ranges. The appropriate parts of the satellite orbits shown in Figure 1 are marked by capital letters. The negative sign means that DEMETER observed individual QP elements later than Kannuslehto.

In order to determine numerically the time delays corresponding to the dependencies from Figure 4, a correlation analysis has been employed. The obtained results are shown in Figure 5. It shows the time delays between the

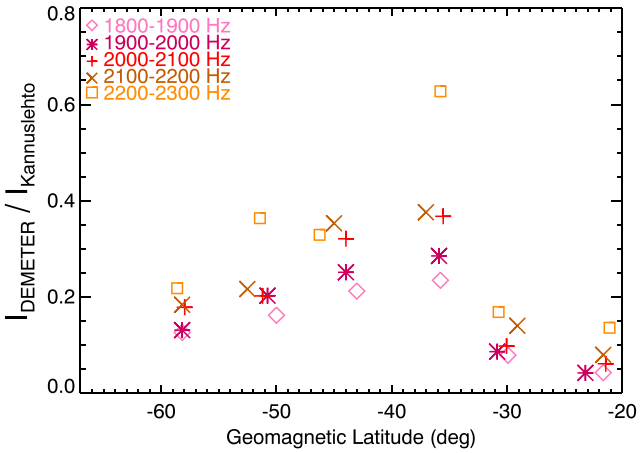


**Figure 6.** Ratio of intensities of QP elements observed by DEMETER and Kannuslehto during the time interval from Figure 4b. Individual color symbols correspond to different frequency ranges, as described in the insert of the figure.

detection of individual QP elements by DEMETER and the Kannuslehto station as a function of frequency. The data points that are plotted by the same symbols of the same color were obtained for the same time interval, but at different frequency ranges. The used time intervals are marked by capital letters, corresponding to the parts of the satellite orbits shown in Figure 1. It can be seen that during the time intervals A and E, the detected time delays were generally very low, below the time resolution of our analysis (approximately 2 s for the DEMETER data and 1 s for the ground-based observations). The time delays detected during the time intervals B, "C," and "D" were significantly larger, as large as about 13 s. The negative sign means that individual QP elements were observed by DEMETER later than by Kannuslehto. Note that the time delay is principally independent of the frequency. Also note that the analysis is performed only in the frequency ranges where the QP emissions are observed with a sufficient intensity both in the DEMETER and ground-based data.

It is of interest to compare the intensity changes of the QP event as observed by DEMETER with the intensity variation observed at Kannuslehto. The idea is that while the observations at Kannuslehto are performed at a fixed location (only rotating along with the Earth), the DEMETER spacecraft moves significantly in the geomagnetic latitude over the course of a few minutes. While the intensity variations observed at Kannuslehto are thus most likely related to the "real temporal variations" of the event, the intensity variations observed by DEMETER are also affected by the spatial effects. We use the intensity observed at Kannuslehto as a normalization factor, and we evaluate the variations of the normalized intensity of QP elements observed by DEMETER as a function of the geomagnetic latitude. The obtained results are shown in Figure 6. The calculation was performed separately for each 100 Hz wide frequency band. The time interval B was used in the analysis, as it is the time interval with the largest number of well-pronounced QP elements. During this time interval, DEMETER was located in the Southern Hemisphere, i.e., in the opposite hemisphere than Kannuslehto. The measurements were performed during a daytime half-orbit when the spacecraft moved from the north to the south; i.e., in Figure 6 decreasing latitudes correspond to increasing times. The results obtained for each of the analyzed frequency bands are plotted by a different color symbol, following the insert at the top left. Six distinct QP elements can be distinguished in the DEMETER data during the analyzed time interval (see Figure 4b); i.e., six intensity ratios were obtained for each frequency band. The intensity of a peak corresponding to a QP element in a given frequency band is defined as the time integral of the wave intensity within the time range corresponding to the duration of a QP element. The duration of a QP element is defined as the time interval between the intensity minima, i.e., between a pair of consecutive same-color crosses in Figure 4b. Note that according to this definition individual QP elements are adjacent to each other.

It can be seen that the results obtained for individual frequency bands are well consistent. The intensity ratios are generally lower than 1, i.e., the power spectral density of electric field fluctuations detected by DEMETER is generally lower than the power spectral density of electric field fluctuations detected by Kannuslehto. This can be, at least in part, explained in terms of a different value of the refractive index. Specifically, while the refractive index at the Kannuslehto station is principally equal to 1, the refractive index at DEMETER altitudes is typically on the order of a few tens. Given that the waves penetrate through the ionosphere down to the ground, we can infer their wave vectors to be nearly vertical. Considering the large geomagnetic latitude of the observations, this means that the corresponding wave normal angles are rather small. For the analyzed time interval and wave normal angles lower than about 60°, the values of refractive index calculated using the cold plasma theory [*Stix*, 1992], in situ measured plasma number densities [*Berthelier et al.*, 2006b], and International Geomagnetic Reference Field (IGRF) magnetic field magnitude are around 30. From the Faraday's

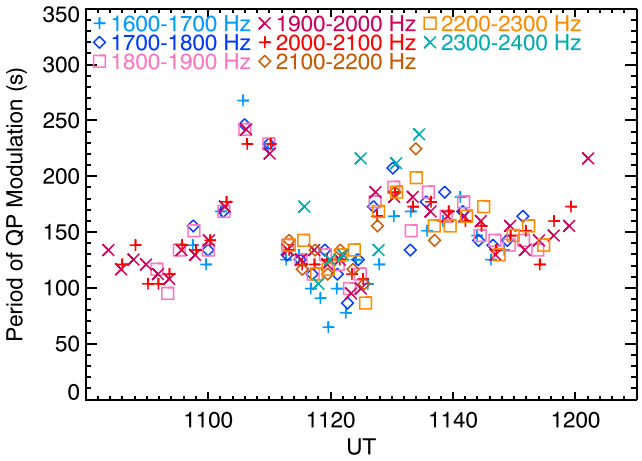


**Figure 7.** Modulation period (i.e., the time separation of two consecutive QP elements) observed by Kannuslehto as a function of time. Individual color symbols correspond to different frequency ranges, following the insert at the top.

law it stems that the wave electric field is related to the wave magnetic field via a factor $c/n$, where $n$ is the refractive index and $c$ is the speed of light. The same Poynting flux of the wave would thus correspond to the electric field power spectral density at DEMETER being about $n$ times lower than at Kannuslehto. Even with a Poynting flux propagated to the ground lower by some 5 dB due to the transionospheric attenuation during the daytime [*Graf et al.*, 2013], we can still obtain the observed value. As the refractive index at DEMETER altitudes in the analyzed frequency range tends to decrease with the wave frequency (by about 10% for the wave frequency of 2250 Hz as compared to the wave frequency of 1850 Hz), this explanation may be possibly also used to at least partly justify why the intensity ratios seem to be larger for higher wave frequencies. The intensity ratio sharply increases at absolute values of geomagnetic latitude of about 35°, and it gradually decreases toward larger geomagnetic latitudes. This indicates that the latitudinal range where the penetration of QP emissions to the low altitudes of the DEMETER spacecraft is the most efficient.

The modulation period of a QP event, i.e., the time separation of consecutive QP elements, can significantly evolve during the time duration of an event [*Němec et al.*, 2013b; *Manninen et al.*, 2013, 2014a]. The time dependence of the modulation period of the analyzed event is shown in Figure 7. Ground-based data measured at the Kannuslehto station have been used, as these are—unlike DEMETER data—continuous in time. Similarly to the aforementioned analysis, the modulation period has been determined independently in 100 Hz wide frequency bands. The results obtained for each of these bands are plotted by a different color

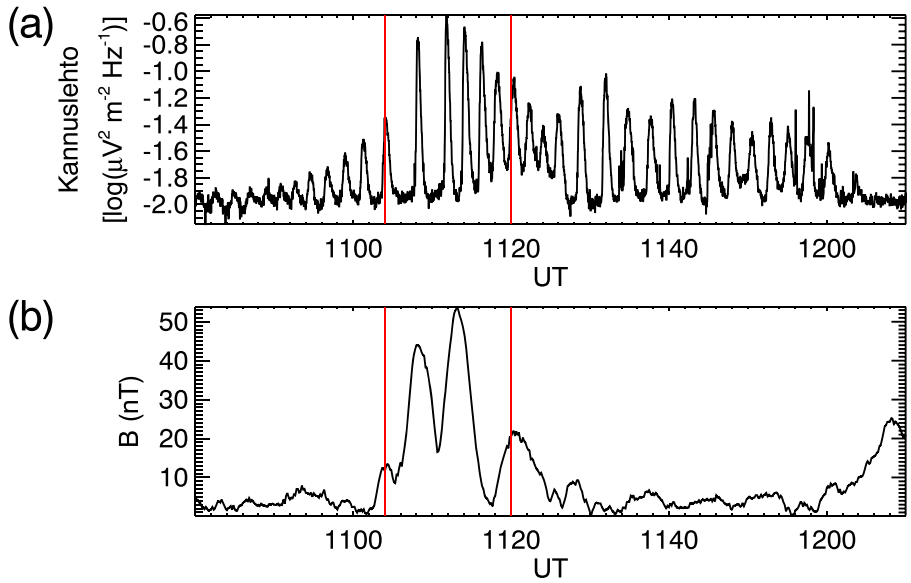


**Figure 8.** (a) Wave intensity detected at Kannuslehto in the frequency range between 1900 Hz and 2000 Hz as a function of time. The vertical red lines mark the time interval when the intensity of the QP emissions suddenly increased. (b) Variation of the magnetic field magnitude perpendicular to the ambient magnetic field detected by the IMAGE magnetometer Ny-Ålesund, Norway (geomagnetic latitude 128.47°, geomagnetic longitude 75.87°) as a function of time. The magnetic field is a maximum at the time interval marked by the vertical red lines.

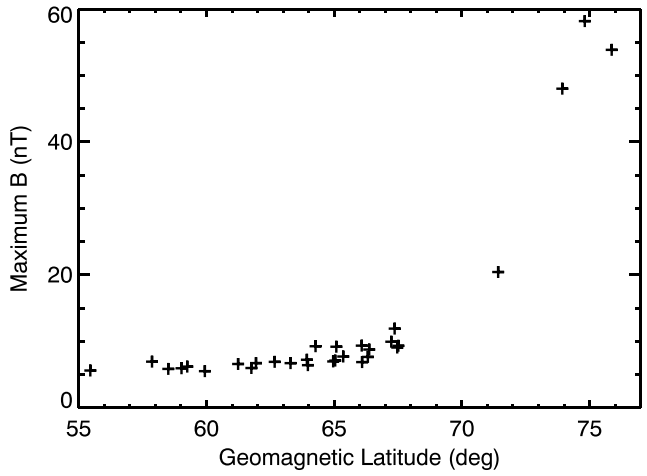


**Figure 9.** Maximum of the magnetic field magnitude perpendicular to the ambient magnetic field detected by the IMAGE magnetometers during the time interval marked by the vertical red lines in Figure 8 as a function of their geomagnetic latitude.

symbol, corresponding to the insert at the top. Note, however, that the modulation period is principally independent of the frequency, as the frequency-time shapes of consecutive QP elements are typically rather similar. It can be seen that while the modulation period is roughly constant in the beginning and in the middle of the event, there are two sudden increases of the modulation period as large as about 100% at about 11:08 UT and 11:34 UT. Moreover, there might be an indication of the third modulation period increase at the very end of the analyzed event (about 12:02 UT).

The time variation of the intensity of QP emissions detected at Kannuslehto is analyzed in Figure 8a, which shows the time dependence of the magnetic field power in the frequency range between 1900 Hz and 2000 Hz by the black curve. It can be seen that the wave intensity in the very beginning of the time interval was very low, and the QP modulation was rather obscured. The intensity of the emissions then gradually increased, and the QP modulation became better pronounced. The intensity of the QP emissions finally decreases toward the end of the analyzed time interval. Importantly, a significant intensity increase is observed at about 11:08 UT, i.e., at the times roughly corresponding to the time of the increase of the modulation period. The time interval when the intensity increase is observed is marked by the red vertical lines.

It is interesting to investigate the variations of the magnetic field pulsations observed on the ground during this time interval. This is done in Figure 8b. We have used the data from the IMAGE magnetometer network, in this particular case the Ny-Ålesund magnetometer in Norway (78.92°N, 11.95°E). The magnetic field magnitude detected on the ground corresponds primarily to the ambient magnetic field, but we are interested in Alfvénic magnetic field pulsations. For this reason, we are interested in the variation of the magnetic field magnitude perpendicular to the ambient magnetic field (determined as the average value during the time interval of 1 h). The obtained time dependence is shown by the black curve. The magnetic field pulsations have a period comparable to the period of the QP modulation, but its relation to the modulation period of QP emissions is inconclusive. Nevertheless, it is noteworthy that the intensity of magnetic field pulsations is maximal during the time interval marked by the red vertical lines.

This phenomenon is investigated in more detail in Figure 9. It focuses exclusively on the time interval marked by the vertical red lines in Figure 8. Then, for each of the IMAGE magnetometer stations, it shows the maximum of the magnetic field magnitude perpendicular to the ambient magnetic field. The results are plotted as a function of the geomagnetic latitude of individual magnetometer stations, which was found to be the main controlling parameter. The maximum magnetic field magnitude is extremely large at high geomagnetic latitudes, and it sharply decreases toward the equator. The increase thus seems to be limited to geomagnetic latitudes larger than about 68°. Converting the geomagnetic latitudes to L shells, assuming a dipole magnetic field approximation, we can conclude that the increase is limited to L shells larger than about 7.1. Note that using the IGRF and T89 [*Tsyganenko*, 1989] magnetic field models to better describe the real magnetic field configuration would only slightly change this L shell estimate (to $L \approx 7.3$).

## 4. Discussion

Multipoint observations of the same event are crucial to distinguish between spatial and temporal variations of the phenomenon. Moreover, the used combination of the low-altitude spacecraft and ground-based measurements has certain considerable advantages. The ground-based measurements provide us with continuous observations of the event performed at the same location, and they therefore allow us to analyze

temporal variations of the event. On the other hand, the DEMETER spacecraft samples a large geographic region within a short time, and it therefore allows us to analyze the spatial variations of the event. The comparison of the locations where the event was observed by DEMETER with the location of the Kannuslehto station indicates that the event is limited to longitudes within about ±90° from the Kannuslehto station. Moreover, sometimes the event is observed by DEMETER at locations very close to Kannuslehto, but it is absent in the Kannuslehto data. This indicates that the waves may have difficulties penetrating from the DEMETER altitudes down to the ground, which seems to be consistent with their unducted propagation [*Němec et al.*, 2013a; *Titova et al.*, 2015; *Hayosh et al.*, 2016].

The time delay between individual QP elements observed at different locations was identified by *Němec et al.* [2014] using the observations performed by the Cluster spacecraft. The reported observations were performed at about the same MLT, but they were separated by as much as 0.5 $R_E$. The observed time delays were on the order of a few seconds, and they were explained by the ray tracing analysis, considering the unducted wave propagation. Conjugate observations of a QP event by the Van Allen Probes and THEMIS spacecraft revealed the time delay as large as 15 s for azimuthal separations of about 25° [*Němec et al.*, 2016]. It was argued that such a large time delay cannot be due to the propagation of the QP emissions. Instead, it was suggested that the time delay might be related to the azimuthal propagation of a modulating ULF wave. The time delays observed in the present study during the time intervals B, C, and D are close to 10 s; i.e., they are also too large to be explained by the propagation of QP emissions themselves. Instead, following *Němec et al.* [2016], we suggest that these time delays might be related to the azimuthal separation of the DEMETER spacecraft and the Kannuslehto station, because of an azimuthally propagating compressional ULF wave, which periodically modulates the source conditions in the source region. This mechanism would also explain how principally the same QP modulation can be generated in an azimuthally extended region. Such an azimuthally extended region seems to be necessary to explain the large azimuthal extent of the event, as propagating whistler mode VLF waves tend to stay within the same magnetic meridian. We note that the mechanism based on the azimuthal propagation of the modulating ULF wave also naturally explains why the observed time delay does not depend on the frequency of the QP emissions. It would be further consistent with apparent fine-scale differences in the inner structure of individual QP elements observed by the satellite and on the ground. However, these might be possibly explained also by different propagation paths in the dispersive plasma medium. Finally, we note that the ground-based observations may be affected by the wave propagation in the Earth-ionosphere waveguide, which also acts to increase the spatial dimensions of the event.

Let us discuss the time delays from Figure 5 in more detail. The time delay during the time intervals A and E was close to 0. At these times, DEMETER was within about 30° in longitude from Kannuslehto. This corresponds to the shortest distance of about 1700 km between the subsatellite magnetic footprint and Kannuslehto. The waves can propagate in the Earth-ionosphere waveguide at such distances, and such a propagation would explain the nearly coincident observation of individual QP elements by DEMETER and the Kannuslehto station. We note that the attenuation of whistler mode waves that couple into the Earth-ionosphere waveguide is expected to be rather large within the first few hundred kilometers [*Nagano et al.*, 1982, 1986]. Experimental analysis suggests that the attenuation rate close to the waveguide entrance point may be as high as about 6–7 dB/100 km [*Tsuruda et al.*, 1982; *Machida and Tsuruda*, 1984]. This large signal attenuation at short distances can be understood in terms of heavily attenuated modes being more efficiently excited [*Barr and Stubbe*, 1984], and it appears to be consistent with the low intensity of event A observed at the Kannuslehto station. The analysis of the azimuth of arrival of these emissions shows that they are coming approximately from the south-west or north-east (it is not possible to resolve the 180° ambiguity using the available data). This roughly corresponds to the direction toward the DEMETER spacecraft, and it is consistent with the suggested picture of the wave propagation in the Earth-ionosphere waveguide. However, after propagating such a long distance in the Earth-ionosphere waveguide, the waves would be expected to have mostly linear polarization [*Tsuruda and Ikeda*, 1979; *Machida and Tsuruda*, 1984]. The waves observed at Kannuslehto are right-hand polarized. This might possibly be due to the polarization-distance dependence being more complicated [*Yearby and Smith*, 1994]. Alternatively, the emissions might get spread over a larger region already in the ionosphere, as suggested by the analysis of whistlers exiting the ionosphere at $L > 6$, although originally ducted at $L \approx 3-4$ [*Strangeways et al.*, 1983].

The time delay during the interval D is about −9 s while DEMETER was closer to Kannuslehto in longitude than in event A. However, during this time interval, the spacecraft was located in the opposite hemisphere.

The observations were performed on the nightside. DEMETER, which was located at later MLTs than Kannuslehto by about 0.7 h (10° in longitude), observed the individual QP elements later. Attributing the observed time delay to an azimuthally propagating ULF wave responsible for the QP modulation, we can estimate its azimuthal speed to be about 1.2°/s. This value is consistent with the value of about 1.5–2°/s estimated by *Němec et al.* [2016]. Moreover, this wave would propagate tailward, which is consistent with ground-based statistical results [*Olson and Rostoker*, 1978; *Chisham and Orr*, 1997] and recent satellite observations [*Takahashi et al.*, 2015a, 2015b]. The longitudinal separation of the orbit parts B and C from the Kannuslehto station is larger than for part D and roughly the same for both events, as are the observed time delays. A direct conversion of the longitudinal separations and observed time delays to azimuthal speeds would for events B and C give values of about 6.3°/s and 5.9°/s, respectively. However, their interpretation is complicated by the fact that while DEMETER was located on the dawnside, Kannuslehto was on the duskside. It is thus well possible that the (hypothetical) modulating ULF wave propagating tailward from the subsolar point would start somewhere between the two observation points. This prevents the azimuthal speed of the wave propagation to be properly determined. We note, however, that a modulating ULF wave starting exactly at the subsolar point would not be consistent with the observed time delays, as during the time interval C DEMETER is by about 40° in azimuth closer to the subsolar point than Kannuslehto, and yet it observes the individual QP elements at later times. It is also noteworthy that even when DEMETER is located on the dawnside and Kannuslehto on the duskside, the frequency-time structure of the event at the two observation points was about the same. This contradicts the observations reported by *Němec et al.* [2016] of the modulation period on the duskside being about twice larger than the modulation period on the dawnside. However, it might possibly be due to the azimuthal separations in the present study not being that large, as compared to nearly 12 h of MLT separation in *Němec et al.* [2016]. Finally, we note once more that the interpretation of the time delays calculated using ground-based data is complicated due to a possible propagation of QP emissions in the Earth-ionosphere waveguide.

The latitudinal dependence of the intensity of QP emissions detected by DEMETER normalized by the intensity of QP emissions detected at Kannuslehto exhibits an increase at absolute values of geomagnetic latitude of about 35°, and it slowly decreases toward larger geomagnetic latitudes. The normalization by the intensity of QP emissions observed at Kannuslehto is assumed to be affected by the same propagation effects for the entire duration of this analysis; i.e., it is considered to correspond to the real time variation of the intensity of the event. The normalization of the QP intensities observed by DEMETER serves to remove this time variation, and it allows us to analyze the spatial variation of the observed intensity. The obtained latitudinal dependence of the intensity of QP emissions observed by DEMETER can be likely explained by the wave propagation from the generation region located at larger radial distances. Specifically, *Hayosh et al.* [2016] reported for other cases that the propagation directions of QP emissions at low altitudes suggest wave guiding along the plasmasphere boundary, with a subsequent deviation toward lower latitudes at low altitudes. According to their results, this deviation appeared to lead the wave primarily to geomagnetic latitudes lower than about 50°. This seems to be roughly consistent with our results.

The period of the QP modulation suddenly increased by as much as 100% around 11:08 UT and 11:34 UT. A possible indication of the third increase of the modulation period was observed at the very end of the analyzed time interval, around 12:02 UT. Although the total duration of the observations is not sufficient to demonstrate this unambiguously, these observations might suggest that the increase of the modulation period is a recurrent phenomenon which occurs every about 25 min. *Manninen et al.* [2013] and *Manninen et al.* [2014a] reported observational evidence that a decrease in the modulation period might be related to substorm injections of energetic electrons. However, there were no substorms taking place during the time interval analyzed in the present paper, and, moreover, we observe a sudden increase of the modulation period, not a decrease. Unfortunately, we were not able to identify the cause of this modulation period increase.

The increase of the magnitude of Alfvénic magnetic field pulsations detected on the ground by the IMAGE magnetometers at high latitudes at the times of the intensity increase of the QP emissions suggests that the two phenomena might be related. There are, however, two principally different possibilities why this should be the case. First, the QP modulation itself might be a result of the source region being periodically modulated by the compressional ULF wave (see above). This ULF wave, compressional close to the geomagnetic equator, might be mode converted to noncompressional Alfvén waves at larger geomagnetic latitudes. The appropriate ULF magnetic field pulsations would be then detected by the magnetometers on the ground. Alternatively, the ULF magnetic field pulsations might be generated in the ionosphere, due to periodic

conductivity changes caused by energetic electrons periodically precipitating due to wave-particle interactions in the source region of QP emissions [*Sato and Matsudo*, 1986]. Such periodic bursts of precipitating energetic electrons were observed along with the QP emissions [*Gołłkowski and Inan*, 2008; *Hayosh et al.*, 2013].

Both mechanisms seem to be capable of explaining the observed dependence. However, if the ULF pulsations were generated by conductivity changes in the ionosphere, one might expect them to be spatially rather limited, principally to the footprints of the magnetic field lines passing through the source region. On the other hand, if the ULF pulsations were in fact a ground-based manifestation of the modulating compressional ULF wave, their spatial extent could be significantly larger. Moreover, there would likely be no sharp on-off transition, but a gradual decrease related to the wave attenuation/lower efficiency of the coupling to the Alfvénic magnetic field line oscillations. The variation obtained in Figure 9 might be possibly consistent with both these explanations. The increase of the magnitude of the Alfvénic magnetic field pulsations is limited to geomagnetic latitudes larger than about 68°, indicating that the QP emissions are generated at L shells larger than about 7.1. We note that the source region located at large L shells would be consistent with no specific extraordinary features identified in DEMETER particle data [*Sauvaud et al.*, 2006] during the time of the QP event (not shown), as these data are generally limited to lower L shells.

## 5. Conclusions

We presented a detailed analysis of conjugate observations of a QP event observed by the DEMETER spacecraft and ground-based instrumentation at the Kannuslehto station, Finland. The observations were performed on 26 February 2008. The event lasted for several hours, and it was detected over a large area both in the Northern and Southern Hemisphere. We have shown that at the times when the event is detected simultaneously by the satellite and on the ground, the observed frequency-time structure is approximately the same. However, the intensity of detected QP elements varied as a function of the geomagnetic latitude of the observer, sharply increasing at about 35° and then slowly decreasing toward larger geomagnetic latitudes. We suggested that this is due to the wave propagation from the source region located at larger radial distances, and the effect of the plasmapause guiding. Moreover, there was a time delay as large as about 13 s between the times when individual QP elements were detected on the ground and by the DEMETER spacecraft. This time delay is too large to be explained by the propagation of whistler mode QP emissions. We suggested that it might be related to an azimuthally propagating compressional ULF wave which is responsible for the generation of QP emissions. The azimuthal speed of this hypothetical ULF wave would have to be on the order of a few degrees per second. Finally, at the times when the intensity of the QP emissions suddenly increased, the amplitude of Alfvénic ULF magnetic pulsations measured on the ground at high latitudes was a maximum. This behavior was not observed by magnetometers located at geomagnetic latitudes lower than about 68°. We argued that this indicates that the source region is located at L shells larger than about 7.1.

**Acknowledgments**
DEMETER was a CNES mission. We thank the engineers from CNES and scientific laboratories (CBK, IRAP, LPC2E, LPP, and SSD of ESTEC) who largely contributed to the success of this mission. DEMETER data are accessible from https://sipad-cdpp.cnes.fr. IMAGE magnetometer data can be downloaded from http://www.ava.fmi.fi/image. We thank the institutes who maintain the IMAGE Magnetometer Array. The work of F.N. and B.B. was supported by GACR grant 15-01775Y and GAUK grant 300216. The work of O.S. was supported by MSMT grant LH 15304, GACR grant 14-31899S, and by the Praemium Academiae award from the CAS.

## References

Barr, R., and P. Stubbe (1984), ELF and VLF radiation from the "polar electrojet antenna", *Radio Sci.*, *19*(4), 1111–1122.
Berthelier, J. J., et al. (2006a), ICE, the electric field experiment on DEMETER, *Planet. Space Sci.*, *54*, 456–471.
Berthelier, J. J., M. Godefroy, F. Leblanc, E. Seran, D. Peschard, P. Gilbert, and J. Artru (2006b), IAP, the thermal plasma analyzer on DEMETER, *Planet. Space Sci.*, *54*, 487–501.
Bespalov, P. A., and V. Y. Trakhtengerts (1976), The dynamics of the cyclotron instability in a magnetic trap, *Fizika Plazmy*, *2*, 397–406.
Carson, W. B., J. A. Koch, J. H. Pope, and R. M. Gallet (1965), Long-period very low frequency emission pulsations, *J. Geophys. Res.*, *70*(17), 4293–4303.
Chen, L. (1974), Theory of ULF modulation of VLF emissions, *Geophys. Res. Lett.*, *1*(2), 73–75.
Chisham, G., and D. Orr (1997), A statistical study of the local time asymmetry of Pc 5 ULF wave characteristics observed at midlatitudes by SAMNET, *J. Geophys. Res.*, *102*(A11), 24,339–24,350.
Davidson, G. T. (1979), Self-modulated VLF wave-electron interactions in the magnetosphere: A cause of auroral pulsations, *J. Geophys. Res.*, *84*(A11), 6517–6523.
Demekhov, A. G., and V. Y. Trakhtengerts (1994), A mechanism of formation of pulsating aurorae, *J. Geophys. Res.*, *99*(A4), 5831–5841.
Engebretson, M. J., J. L. Posch, A. J. Halford, G. A. Shelburne, A. J. Smith, M. Spasojević, U. S. Inan, and R. L. Arnoldy (2004), Latitudinal and seasonal variations of quasiperiodic and periodic VLF emissions in the outer magnetosphere, *J. Geophys. Res.*, *109*, A05216, doi:10.1029/2003JA010335.
Fedorenko, Y., E. Tereshchenko, S. Pilgaev, V. Grigoryev, and N. Blagoveshchenskaya (2014), Polarization of ELF waves generated during "beating-wave" heating experiment near cutoff frequency of the Earth-ionosphere waveguide, *Radio Sci.*, *49*, 1254–1264, doi:10.1002/2013RS005336.
Gołłkowski, M., and U. S. Inan (2008), Multistation observations of ELF/VLF whistler mode chorus, *J. Geophys. Res.*, *113*(A08210), doi:10.1029/2007JA012977.

Graf, K. L., N. G. Lehtinen, M. Spasojevic, M. B. Cohen, R. A. Marshall, and U. S. Inan (2013), Analysis of experimentally validated trans-ionospheric attenuation estimates of VLF signals, *J. Geophys. Res. Space Physics*, *118*, 2708–2720, doi:10.1002/jgra.50228.

Hayosh, M., D. L. Pasmanik, A. G. Demekhov, O. Santolík, M. Parrot, and E. E. Titova (2013), Simultaneous observations of quasi-periodic ELF/VLF wave emissions and electron precipitation by DEMETER satellite: A case study, *J. Geophys. Res. Space Physics*, *118*, 4523–4533, doi:10.1002/jgra.50179.

Hayosh, M., F. Němec, O. Santolík, and M. Parrot (2014), Statistical investigation of VLF quasiperiodic emissions measured by the DEMETER spacecraft, *J. Geophys. Res. Space Physics*, *119*, 8063–8072, doi:10.1002/2013JA019731.

Hayosh, M., F. Němec, O. Santolík, and M. Parrot (2016), Propagation properties of quasi-periodic VLF emissions observed by the DEMETER spacecraft, *J. Geophys. Res. Space Physics*, *43*, 1007–1014, doi:10.1002/2015GL067373.

Inan, U. S., and T. F. Bell (1977), The plasmapause as a VLF wave guide, *J. Geophys. Res.*, *82*(19), 2819–2827.

Kimura, I. (1974), Interrelation between VLF and ULF emissions, *Space Sci. Rev.*, *16*, 389–411.

Kitamura, T., J. A. Jacobs, T. Watanabe, and J. R. B. Flint (1969), An investigation of quasi-periodic VLF emissions, *J. Geophys. Res.*, *74*(24), 5652–5664.

Machida, S., and K. Tsuruda (1984), Intensity and polarization characteristics of whistlers deduced from multi-station observations, *J. Geophys. Res.*, *89*(A3), 1675–1682.

Manninen, J. (2005), *Some Aspects of ELF-VLF Emissions in Geophysical Research*, chap. Magnetospheric Line Radiation, vol. 98, 85–110 pp., Sodankylä Geophysical Observatory Publ., Sodankylä,Finland.

Manninen, J., N. G. Kleimenova, and O. V. Kozyreva (2012), New type of ensemble of quasi-periodic, long-lasting VLF emissions in the auroral zone, *Ann. Geophys.*, *30*, 1655–1660, doi:10.5194/angeo-30-1655-2012.

Manninen, J., N. G. Kleimova, O. V. Kozyreva, P. A. Bespalov, and A. E. Kozlovsky (2013), Non-typical ground-based quasi-periodic VLF emissions observed at $L \sim 5.3$ under quiet geomagnetic conditions at night, *J. Atmos. Sol. Terr. Phys.*, *99*, 123–128.

Manninen, J., A. G. Demekhov, E. E. Titova, A. E. Kozlovsky, and D. L. Pasmanik (2014a), Quasiperiodic VLF emissions with short-period modulation and their relationship to whistlers: A case study, *J. Geophys. Res. Space Physics*, *119*, 3544–3557, doi:10.1002/2013JA019743.

Manninen, J., E. E. Titova, A. G. Demekhov, A. E. Kozlovskii, and D. L. Pasmanik (2014b), Quasiperiodic VLF emissions: Analysis of periods on different timescales, *Cosmic Res.*, *52*(1), 61–67, doi:10.1134/S0010952514010055.

Martinez-Calderon, C., et al. (2016), ELF/VLF wave propagation at subauroral latitudes: Conjugate observation between the ground and Van Allen Probes A, *J. Geophys. Res. Space Physics*, *121*, 5384–5393, doi:10.1002/2015JA022264.

Morrison, K. (1990), Quasi-periodic VLF emissions and concurrent magnetic pulsations seen at $L = 4$, *Planet. Space Sci.*, *38*(12), 1555–1565.

Morrison, K., M. J. Engebretson, J. R. Beck, J. E. Johnson, R. L. Arnoldy, J. L. J. Cahill, D. L. Carpenter, and M. Gallani (1994), A study of quasi-periodic ELF-VLF emissions at three Antarctic stations: Evidence for off-equatorial generation?, *Ann. Geophys.*, *12*, 139–146, doi:10.1007/s00585-994-0139-8.

Nagano, I., M. Mambo, S. Yoshizawa, I. Kimura, and H. Yamagishi (1982), Full wave calculation for a Gaussian VLF wave injection into the ionosphere, *Mem. Natl Inst. Polar Res. Spec. Issue*, *22*, 46–57.

Nagano, I., M. Mambo, T. Shimbo, and I. Kimura (1986), Intensity and polarization characteristics along the Earth's surface for the ELF-VLF waves emitted from a transmission cone in the high latitude, *Mem. Natl Inst. Polar Res. Spec. Issue*, *42*, 34–44.

Němec, F., O. Santolík, J. S. Pickett, M. Parrot, and N. Cornilleau-Wehrlin (2013a), Quasiperiodic emissions observed by the Cluster spacecraft and their association with ULF magnetic pulsations, *J. Geophys. Res. Space Physics*, *118*, 4210–4220, doi:10.1002/jgra.50406.

Němec, F., O. Santolík, M. Parrot, J. S. Pickett, M. Hayosh, and N. Cornilleau-Wehrlin (2013b), Conjugate observations of quasi-periodic emissions by Cluster and DEMETER spacecraft, *J. Geophys. Res. Space Physics*, *118*, 198–208, doi:10.1029/2012JA018380.

Němec, F., J. S. Pickett, and O. Santolík (2014), Multispacecraft Cluster observations of quasiperiodic emissions close to the geomagnetic equator, *J. Geophys. Res. Space Physics*, *119*, 9101–9112, doi:10.1002/2014JA020321.

Němec, F., G. Hospodarsky, J. S. Pickett, O. Santolík, W. S. Kurth, and C. Kletzing (2016), Conjugate observations of quasiperiodic emissions by the Cluster, Van Allen Probes, and THEMIS spacecraft, *J. Geophys. Res. Space Physics*, *121*, 7647–7663, doi:10.1002/2016JA022774.

Olson, J. V., and G. Rostoker (1978), Longitudinal phase variations of PC 4–5 micropulsations, *J. Geophys. Res.*, *83*(A6), 2481–2488.

Pasmanik, D. L., A. G. Demekhov, V. Y. Trakhtengerts, and M. Parrot (2004a), Modeling whistler wave generation regimes in magnetospheric cyclotron maser, *Ann. Geophys.*, *22*, 3561–3570.

Pasmanik, D. L., E. E. Titova, A. G. Demekhov, V. Y. Trakhtengerts, O. Santolik, F. Jiricek, K. Kudela, and M. Parrot (2004b), Quasi-periodic ELF/VLF wave emissions in the Earth's magnetosphere: Comparison of satellite observations and modelling, *Ann. Geophys.*, *22*, 4351–4361.

Sato, N., and H. Fukunishi (1981), Interaction between ELF-VLF emissions and magnetic pulsations: Classification of quasi-periodic ELF-VLF emissions based on frequency-time spectra, *J. Geophys. Res.*, *86*(A1), 19–29.

Sato, N., and S. Kokubun (1980), Interaction between ELF-VLF emissions and magnetic pulsations: Quasi-periodic ELF-VLF emissions associated with Pc 3–4 magnetic pulsations and their geomagnetic conjugacy, *J. Geophys. Res.*, *85*(A1), 101–113.

Sato, N., and T. Matsudo (1986), Origin of magnetic pulsations associated with regular period VLF pulsations (Type 2 QP) observed on the ground at Syowa station, *J. Geophys. Res.*, *91*(A10), 11,179–11,185.

Sato, N., K. Hayashi, S. Kokubun, T. Oguti, and H. Fukunishi (1974), Relationships between quasi-periodic VLF emission and geomagnetic pulsation, *J. Atmos. Terr. Phys*, *36*, 1515–1526.

Sauvaud, J. A., T. Moreau, R. Maggiolo, J.-P. Treilhou, C. Jacquey, A. Cros, J. Coutelier, J. Rouzaud, E. Penou, and M. Gangloff (2006), High-energy electron detection onboard DEMETER: The IDP spectrometer, description and first results on the inner belt, *Planet. Space Sci.*, *54*, 502–511.

Sazhin, S. S. (1987), An analytical model of quasiperiodic ELF-VLF emissions, *Planet. Space Sci.*, *35*(10), 1267–1274.

Sazhin, S. S., and M. Hayakawa (1994), Periodic and quasiperiodic VLF emissions, *J. Geophys. Res.*, *56*(6), 735–753.

Smith, A. J., D. L. Carpenter, Y. Corcuff, J. P. S. Rash, and E. A. Bering (1991), The longitudinal dependence of whistler and chorus characteristics observed on the ground near $L = 4$, *J. Geophys. Res.*, *96*(A1), 275–284, doi:10.1029/90JA01077.

Smith, A. J., M. J. Engebretson, E. M. Klatt, U. S. Inan, R. L. Arnoldy, and H. Fukunishi (1998), Periodic and quasiperiodic ELF/VLF emissions observed by an array of Antarctic stations, *J. Geophys. Res.*, *103*(A10), 23,611–23,622.

Stix, T. H. (1992), *Waves in Plasmas*, Chap. Wave Normal Surfaces, Waves in a Cold Uniform Plasma, 1–46 pp., Springer, New York.

Strangeways, H. J., M. A. Madden, and M. J. Rycroft (1983), High latitude observations of whistlers using three spaced goniometer receivers, *J. Atmos. Terr. Phys*, *45*(6), 387–399, doi:10.1016/S0021-9169(83)81098-8.

Takahashi, K., R. E. Denton, W. Kurth, C. Kletzing, J. Wygant, J. Bonnell, L. Dai, K. Min, C. W. Smith, and R. MacDowall (2015a), Externally driven plasmaspheric ULF waves observed by the Van Allen Probes, *J. Geophys. Res. Space Physics*, *120*, 526–552, doi:10.1002/2014JA020373.

Takahashi, K., M. D. Hartinger, V. Angelopoulos, and K.-H. Glassmeier (2015b), A statistical study of fundamental toroidal mode standing Alfvén waves using THEMIS ion bulk velocity data, *J. Geophys. Res. Space Physics*, *120*, 6474–6495, doi:10.1002/2015JA021207.

Tanskanen, E. I. (2009), A comprehensive high-throughput analysis of substorms observed by IMAGE magnetometer network: Years 1993–2003 examined, *J. Geophys. Res.*, *114*, A05204, doi:10.1029/2008JA013682.

Titova, E. E., B. V. Kozelov, A. G. Demekhov, J. Manninen, O. Santolík, C. A. Kletzing, and G. Reeves (2015), Identification of the source of quasiperiodic VLF emissions using ground-based and Van A llen probes satellite observations, *Geophys. Res. Lett.*, *42*, 6137–6145, doi:10.1002/2015GL064911.

Tixier, M., and N. Cornilleau-Wehrlin (1986), How are the VLF quasi-periodic emissions controlled by harmonics of field line oscillations? The results of a comparison between ground and GEOS satellites measurements, *J. Geophys. Res.*, *91*(A6), 6899–6919.

Trakhtengerts, V. Y., V. R. Tagirov, and S. A. Chernous (1986), Flow cyclotron maser and impulsive VLF emissions, *Geomagn. Aeron.*, *26*, 99–106.

Tsuruda, K., and M. Ikeda (1979), Comparison of three different types of VLF direction-finding techniques, *J. Geophys. Res.*, *84*(A9), 5325–5332.

Tsuruda, K., S. Machida, T. Terasawa, and A. Nishida (1982), High spatial attenuation of the Siple transmitter signal and natural VLF chorus observed at ground-based chain stations near Roberval, Quebec, *J. Geophys. Res.*, *87*(A2), 742–750.

Tsyganenko, N. A. (1989), A magnetospheric magnetic field model with a warped tail current sheet, *Planet. Space Sci.*, *37*(1), 5–20.

Yearby, K. H., and A. J. Smith (1994), The polarisation of whistlers received on the ground near $l = 4$, *J. Atmos. Terr. Phys*, *56*(11), 1499–1512.